4626_4DlHsul7XCIQcIZIHmx4.docx

By Turnitin

WORD COUNT	7035	TIME SUBMITTED	13-DEC-2025 11:12AM
		PAPER ID	119448089

Growth and Reaction Mechanism of Solution-Processed $Cu_2ZnSnSe_4$ (CZTSe) Thin Films for Realizing Efficient Photovoltaic applications

Ersan Y. Muslih[1,8*], K. Sobayel [2*], Mohammad Ismail Hossain[3], Mohammad Junaebur Rashid[4,5], Hend I. Alkhammash[6], Badrul Munir[7], Md. Shahiduzzaman[8], Md. Akhtaruzzaman [2], Kim Kyoo Ho [9], Tetsuya Taima[8]

[1]Mechanical Engineering Department, Faculty of Industrial Technology, Trisakti University, Jakarta 11440. Indonesia
[2] Solar Energy Research Institute, The National University of Malaysia, 43600 Bangi, Selangor, Malaysia
[3]Department of Materials Sciences and Engineering, City University of Hong Kong, Kowloon, Hong Kong
[4]Department of Electrical and Electronic Engineering, University of Dhaka, Dhaka 1000, Bangladesh
[5]Semiconductor Technology Research Center, University of Dhaka, Dhaka 1000, Bangladesh
[6]Department of Electrical Engineering, College of Engineering, Taif University, P.O.Box 11099, Taif 21944, Saudi Arabia
[7]Department of Metallurgy and Materials Engineering, Universitas Indonesia, Depok, Indonesia
[8]Graduate School of Natural Science and Technology, Kanazawa University, Kakuma, Kanazawa 920-1292, Japan
[9]School of Material Science and Engineering, Yeungnam University, 214-1 Daedong, Gyeongsan, Gyeongbuk 712-749, South Korea.

Corresponding author: ersan.ym@trisakti.ac.id.; sobayel@ukm.edu.my; shahiduzzaman@se.kanazawa-u.ac.jp

Abstract

The $Cu_2ZnSnSe_4$ (CZTSe) thin films were successfully grown by a non-hydrazine, non-pyridine, low-cost, and friendly environmentally solution process from CZT (Cu, Zn, and Sn) film precursor and continued with selenization. The CZT film precursor was prepared from the deposition of the CZT solution precursor on sodalime glass (SLG) that made from metal salts (Cu^{2+}, Zn^{2+}, and Sn^{4+}) in monoethanolamine (MEA) and ethanol mixture solvent then followed by annealing at 200 °C for 15 minutes under ambient atmosphere. Furthermore, selenium was added to the CZT film precursor by selenization under Ar (95%) + H_2 (5%) atmosphere at 550 °C for 120 minutes. The growth and reaction mechanism, including metals and carbon contain from precursors and solvents residue, also explained. The result shows the CZTSe thin film was completely formed with high crystallinity, no carbon residue,

Formatted: Shadow

and has suitable optoelectrical properties as absorber layer in solar cells. Finally, simulation study endorses that material properties of as grown CZTSe film can provide a major breakthrough for kesterite thin film solar cell and can exhibit the efficiency upto 23.88%.

Keywords: CZTSe, monoethanolamine, non-hydrazine, CZT film precursor, CZT solution precursor, spin coating, selenization.

Introduction

The kesterite solar cells such as Cu_2ZnSnS_4 (CZTS), $Cu_2ZnSnSe_4$ (CZTSe), and $Cu_2ZnSn(S,Se)_4$ are the most promising absorber materials for solar cell applications today due to earth-abundant and low-cost fabrication. ~~Nowadays, The~~ best power efficiency solar cell for kesterite thin film such as ~~Cu_2ZnSnS_4~~ CZTS thin films could reach 11.01 % by evaporation [1], whereas ~~$Cu_2ZnSnSe_4$~~ CZTSe and $Cu_2ZnSn(S,Se)_4$ by hydrazine addition had an efficiency of 10.54 % and 12.6 % respectively [2,3]. ~~The kesterite solar cells such as CZTS, CZTSe, and CZTSSe are the most promising absorber materials for solar cell applications today due to earth-abundant and low-cost fabrication.~~

CZTSe solar cells can be made using thermal evaporation, sputtering, electrodeposition, and solution technique [4-10]. However, the CZTSe solar cell's prominent efficiency was made by a solution technique using hydrazine as a solvent [3]. Hydrazine is a non-carbon organic compound that can act as a solvent for many organic or inorganic compounds. Because of its unique property, hydrazine is a prominent solvent to synthesized selenium-based kesterite such as CZTSe due to it makes a high grain and uniformity of layer properties and low wastage of raw materials [11,12]. Moreover, hydrazine also has an important role as a catalyst and reducing agent, which can accelerate the synthesis of CZTSe, and it may lead to CZTSe thin film has a high performance [13,14]. However, deposition using a hydrazine solvent also has some disadvantages, such as flammable, corrosive, acutely toxic, carcinogenic, and environmentally hazardous. Hydrazine is a very unstable compound that requires

rigorous safety protocols. The vapor of pure hydrazine may explode if ignited and incompatible with several materials, including many plastics and metals [15-17]. All of these disadvantages are in contrast with environmentally friendly and difficult to make a large scale of production.

Not many alternative solution techniques to synthesis CZTSe non-hydrazine have been developed. Also not many papers perform the fabrication of CZTSe by selenourea, sodium selenite, and selenium dioxide [18-20]. Nevertheless However, the reagents mentioned above are a lot of disadvantages. The reagent selenourea can be dissolved in the water, but it is almost twenty times more expensive than sodium selenite or selenium in pellet form. On the other hand, sodium selenite is cheaper than selenourea, but it cannot easily make some reactions with Cu^{2+}, Zn^{2+}, and Sn^{4+} due to selenium in sodium selenite has selenium as 4+ charge. Obviously, it cannot make any reaction with Cu^{2+}, Zn^{2+}, and Sn^{4+} ions unless a strong reducing agent such as pyridine added into the solution that can change Se^{4+} to Se^{2-}. Pyridine is suitable for this solution technique because non or less carbon content, non-metal content and can mix with Cu, Zn, and Sn [21-23]. However, not an easy task handing pyridine due to pyridine as it is a toxic, flammable, irritant and carcinogenic agent [24-26].

Thus, in this work we introduce a new non-hydrazine, low-cost and environmentally friendly solution technique to synthesized CZTSe thin films. This technique consists of two steps. The first step is making a CZT film precursor by depositing and annealing a solution that contains Cu^{2+}, Zn^{2+}, and Sn^{4+} on the sodalime glass (SLG). And the second step was reacting to the CZT film precursor with selenium pellets by selenization process to obtain CZTSe thin film. The CZT solution was made by dissolving Cu, Zn, and Sn salts in monoethanolamine (MEA) and ethanol. Afterwards, Fourier transform infrared (FTIR) and Raman characterization confirms . And the CZTSe thin films confirmed by Raman spectra. A complete reaction mechanism was investigated in this work including the chemical composition. Also, the and optoelectrical properties of CZTSe thin film as an absorber layer in CZTSe solar cells is studied.

Experimental Details

Soda-lime glass (SLG) preparation

Soda-lime glass (SLG) was cleaned by an ultrasonic water bath in acetone, ethanol, and deionized water for 20 minutes, respectively.

CZT (Cu, Zn, Sn) film precursor

The CZT (Cu, Zn, and Sn) film precursor was made from annealed of CZT solution precursor that prepared from Cu^{2+}, Zn^{2+}, and Sn^{4+} metal salts such as copper (II) acetate monohydrate, zinc acetate dihydrate, and tin (IV) chloride dihydrate were purchased from Sigma Aldrich. All metal salts were separately dissolved by ultrasonic-assisted in 10 mL ethanolamine, which also purchased from Sigma Aldrich with the concentration of Cu, Zn and Sn elements were 0.0750 M, 0.0500 M, and 0.0500 M, respectively. After each metal salts were completely dissolved in monoethanolamine (MEA), all those solutions were mixed until the solution's color was a dark blue solution. And then, ethanol was added until the solution's volume was 100 mL and stirred until homogeneous. Moreover, the CZT precursor solution was deposited using spin coating at 2000 rpm for 15 seconds on 2.5 cm × 2.5 cm soda-lime glass (SLG) and then annealed under an ambient atmosphere at 200 °C for 10 minutes in the tubular heater until black-brownish film color obtained.

Growth of CZTSe thin film

The CZTSe thin films obtained by adding selenium into the CZT precursor through selenization under Ar (95%) and H_2 (5%) mix gases at 550 °C for 120 minutes with 10 sccm of flow rate. After selenization, the sample was cooled to room temperature under natural conditions.

Characterization of CZTSe thin films

The microstructural and cross-section analysis of films ~~was~~ were determined under the scanning electron microscope (SEM) by Hitachi (S 4800, Japan), with an operating voltage of 15 kV. While compositional analysis of films was examined using the energy dispersive x-ray (EDX) by Horiba, Japan attached to the respective SEM apparatus with an acceleration voltage, working distance, and

emission current of 15 kV, 15 mm, and 10 µA, respectively. The crystallinity and structural analysis performed under x-ray diffractometer (XRD) by Rigaku (DMAX 2500, Japan) with fixed angle 2θ, and λ = 1.5405 Å. The measurement conditions were performed at 40 kV, 100 mA, scan speed 2θ with diffraction angle 2θ between 1° and 65°. The complimentary XRD data was obtained by Renishaw (REO2, U.K.) micro-Raman spectroscopy at 514.5 nm using Ar ion C.W. laser. The spectra absorption was recorded by Varian (Carry 5000, USA) UV-Vis-NIR Spectrophotometer in the wavelength range 300 - 1500 nm. Electrical properties were determined by Ecopia (HMS-300, USA) Hall-Effect measurement at 0.01 µA. The thermal study of CZT precursor and organic compound decomposition were characterized by differential scanning calorimetry (Q200, USA) and supported with Fourier transform infra-red (FTIR) data by Perkin Elmer (C86199, USA).

Results and Discussion

In this work, CZTSe thin film was made by a two-step reaction. The first step is making a CZT solution precursor from Cu^{2+}, Zn^{2+}, and Sn^{4+} metal salts using monoethanolamine (MEA) and ethanol as mixed solvents. At this point, monoethanolamine acts as a chelating / complexant [27] and making coordination compound with Cu^{2+}, Zn^{2+}, and Sn^{4+} metal salts. The complex compounds were indicated by the dark blue color of the solution representing the copper-monoethanolamine complex compound, while zinc and tin-monoethanolamine complex compounds showed a transparent solution, respectively.

However, since monoethanolamine has a high surface tension, it makes monoethanolamine difficult to evaporate and attached to the substrate. Thus, to reduce monoethanolamine's surface tension and increase its wet ability, the metal salts-monoethanolamine complex compounds were mixed with ethanol until the ratio 30:70 between metal salts-monoethanolamine and ethanol, respectively. This solution named as the CZT precursor and it is a stable solution ~~because of~~ as the metal salts-monoethanolamine coordination compound has been formed. Its coordination compound bonding had stronger bonding than metal-hydroxyl in ethanol and makes the mixture remain stable. This coordination mechanism is visualized in figure 1.

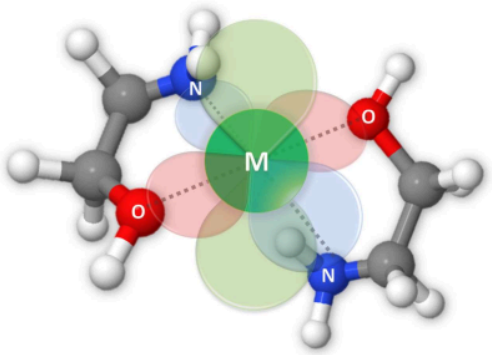

Figure 1. Metal-monoethanolamine complex compound structure.

~~Moreover, the CZT solution precursor was a deposit, annealed and followed by selenization to obtained CZTSe thin film. All of these steps were described concisely in figure 2.~~ Meanwhile, the chemical composition of the CZT solution was made as Cu/(Zn+Sn) ratio and Zn/Sn ratio as 0.75 and 1.00, respectively. This condition is ~~called~~ known as ~~a~~ copper-poor zinc-rich condition. ~~and this condition~~ It was intentionally made~~, and~~ as ~~it~~ this is the optimum condition to ~~aiming~~ obtain CZTSe thin film containing copper poor zinc-rich at the final process. ~~At this point,~~ The CZTSe thin film grown in this way can ~~give a~~ exhibit good performance as an absorber layer leading to ~~and makes its~~ efficient solar cells ~~have a better performance~~ [28-30].

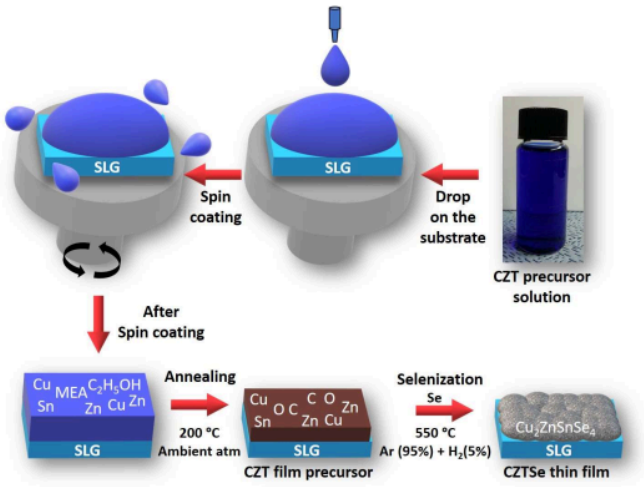

Figure 2. Schematic diagram of synthesizing CZTSe thin film from CZT precursor.

The CZT solution precursor deposition and annealing followed by selenization to obtain CZTSe thin film were described concisely in figure 2. At first ~~Moreover~~, the CZT solution precursor was deposited on SLG by spin coater 2000 rpm for 15 seconds ~~and~~ followed by an annealing at 200 °C for 15 minutes. At this step, metal-ethanolamine complex compounds were slightly to decompose. During decomposition, intermetallic atoms make a binary alloy, whereas organic compounds such as acetate, ethanol, and ethanolamine decompose partially into organic residues such as C or C.O. as amorphous substances which deposited along with Cu and intermetallic binary alloy. The reaction of Cu, Zn, and Sn in the metal salts with MEA until annealing process are:

$$M^{x+}\ (aq) + MEA\ (l) \rightarrow M[MEA]_x\ (aq) \quad (1)$$

$$M[MEA]_x\ (aq) \rightarrow M\ (s) + Organic\ residue\ (s) \quad (2)$$

$$Cu\ (s) + Zn\ (s) \rightarrow Cu_xZn_y\ (s) \quad (3)$$

$$Cu\ (s) + Sn\ (s) \rightarrow Cu_xSn_y\ (s) \quad (4)$$

~~W~~where, M = Cu, Zn and Sn.

After annealing, the CZT precursor film showing two peaks in the XRD pattern as shown in Figure 3,

which were indexed as 111 and 200. Both peaks are probably exhibited in copper, and intermetallic binary alloy peaks such as Cu_xZn_y and Cu_xSn_y which are surrounded by organic amorphous residue ~~as amorphous~~, shown as a broad 2θ peak below 35°. Both ~~of~~ intermetallic compounds are possible to form below 200 °C according to Cu, Zn, and Sn ternary phase diagram. However, there was no evidence for the Zn_xSn_y compound or even metal oxide from the metal-monoethanolamine complex compound due to the preferential reaction between zinc and tin with copper. This initial chemical composition of the CZT precursor also has a similar result with research conducted by Wibowo *et al*. for Cu-Zn-Sn alloy as a precursor for CZTSe thin film [31]. In this work, we made the chemical composition Cu, Zn, and Sn of 45 %, 30 %, and 25 %, respectively with Cu/(Zn+Sn) ratio 0.82. This XRD pattern shows matching with the Cu-Zn-Sn ternary phase diagram in Figure 3.

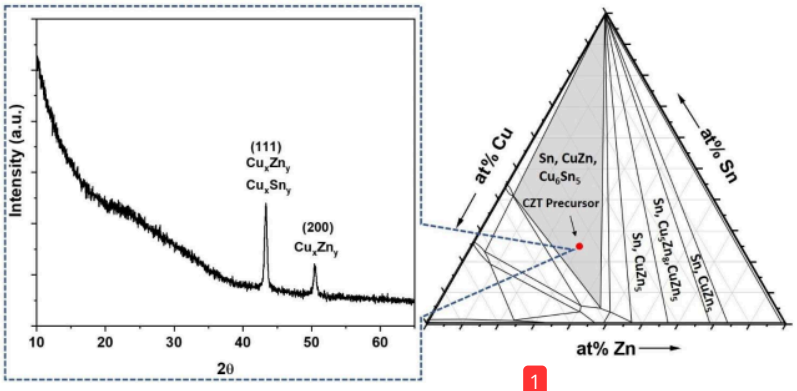

Figure 3. XRD pattern of CZT precursor after annealing at certain composition in the Cu-Zn-Sn ternary phase diagram.

Besides inorganic compounds, this work also involves organic compounds such as acetate from metal salts, ethanol, and MEA as solvents that can leave organic residue in the film as carbon or graphite. Thus, this organic residue could be traced by FTIR and Raman as well. The FTIR spectrum of the CZT precursor before drying shows the spectrum in Figure 4. There were peaks at 1365 cm^{-1}, and 1469 cm^{-1} are shown a CH_2 and CH_3 group peaks in the ethanol, respectively. However, besides showing a peak

for the CH_3 group in the ethanol, peak at 1469 cm^{-1} also showing the CH_2 group in the ethanolamine. A broad peak at 3353 cm^{-1} shows a peak for hydroxyl influenced by hydrogen bonding from the solvent. The peaks at 3287 cm^{-1}, 1078 cm^{-1}, and 1032 cm^{-1}, and peak at 1592 cm^{-1} belonging to N-H peaks However, this peak is a specific indication ~~for~~ of the aliphatic amine group. The exhibited peaks at 2932 cm^{-1} and 2869 cm^{-1} ~~were an exhibit~~ confirms the ~~for~~ hydrocarbon (C-H) bonding. Overall, the spectrum of CZT precursors in the solution phase was dominated by the ethanolamine spectrum due to ethanol had a similarity molecule with ethanolamine. Therefore, ethanol peaks were covered by ethanolamine peaks. After annealing, the CZT precursor shows a different spectrum from the CZT precursor in the solution phase, which could be shifted, decreased the intensity, or even disappeared. These conditions are evidence that organic compounds in the CZT precursor were decomposed partially. However, because of monoethanolamine has amine and hydroxyl as active sites, both sites could react and make some compounds during calcination that can be identified as the broad peak at 3422 cm^{-1}, which exhibit for hydroxyl site (-OH) from ester without hydrogen bonding between ligand and solvent, peak at 2215 cm^{-1} was specifically represent ~~of~~ nitrile group, peaks at 2932 and 2869 cm^{-1} were representing ~~of~~ C-H bonding that still existing even after annealing. Furthermore, shoulder peaks at 1700 cm^{-1} and 1627 cm^{-1} were representing ~~of~~ C=O bonding and ~~also~~ N-H group, respectively. Nevertheless, after calcination, the CZT precursor condition is sufficient to prevent oxidation in the CZT film precursor due to oxidation in the ligand. This result was consistent with TGA-DSC data, which shows dihydroxylation and decomposition partially in the CZT precursor thin film. On the other hand, in the figure 4b, shows Raman spectra before annealing, that exhibits specific for the Cu, Zn, and Sn salts in the monoethanolamine. However, after annealing Raman spectra completely changed that exhibits D and G peaks at 1350 cm^{-1} and 1585 cm^{-1}, respectively. It is clearly shown that almost every organic compound has decomposed into carbon that majority as graphite compound showing a specific pattern for the Cu, Zn, and Sn salts in the monoethanolamine. However, after annealing Raman spectra completely changed that exhibits D and G peaks at 1350 cm^{-1} and 1585 cm^{-1}, respectively. It

is clearly shown that almost every organic compound has decomposed into carbon that majority as graphite compound. Figure 4 shows Fourier transform infra-red (FTIR) and Raman spectroscopy of the CZT precursor before and after annealing.

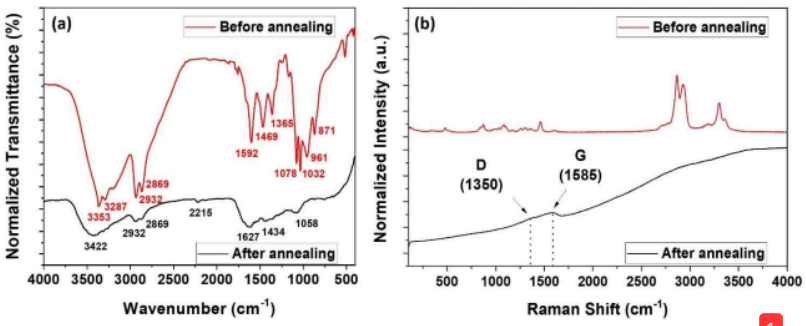

Figure 4. Fourier transform infrared (FTIR) spectrum (a) and Raman spectroscopy (b) of CZT precursor before and after annealing

~~Moreover,~~ The thermal properties of the CZT precursor were studied by thermal gravimetry – differential scanning calorimetry (TG-DSC), as shown in Figure 5. When the temperature exceeded 200 °C, the T.G. graphic shows a significant decrease until around 400 °C. This phenomenon indicates further decomposition of organic residues and ~~the~~ rest of the organic compounds. From its derivative weight could be seen the decomposition by a high derivative of weight from 200 °C to 500 °C. On the other hand, the DSC curve also clearly seen the decomposition phenomenon showing a significant decreasing trend or endothermic trend from 400 °C to 600 °C. However, at 300 °C to 350 °C, it shows a slight exothermic peak ~~due to~~ which corresponds to binary alloy formation such as CuZn and CuSn. The partial decomposition phenomenon of the CZT precursor also could be confirmed by ~~Fourier transform infra-red~~ FTIR characterization in the Figure 4a. This spectrum indicates that the thin film was shrinking due to releasing some organics ~~residues~~. Figure 5 shows TGA-DSC graphic of CZT precursor at 27 °C – 500 °C under ambience atmosphere.

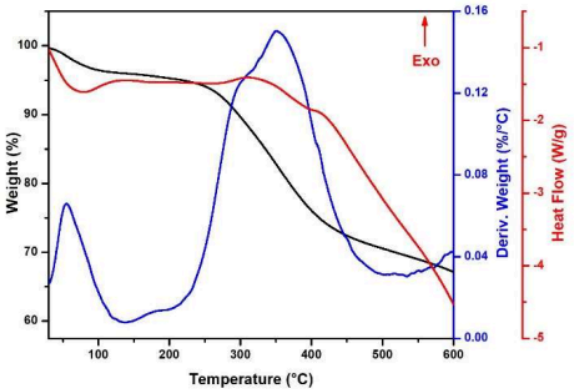

Figure 5. TGA-DSC graphic of CZT precursor at 27 °C – 500 °C.

The XRD pattern of CZT precursors at elevated selenization temperature is shown in Figure 6. ~~Furthermore,~~ In the selenization process at 250 °C, the CZT precursor was reacted with selenium, which already evaporated in small amounts to form SnSe, which marked as a peak at 2θ = 31.37° and also probably there was CuSe which marked on a small peak at 2θ = 25.63°. Besides, CuSe and SnSe, at this condition, also there is a formation of ~~occur~~ Cu_xZn_y and Cu_xSn_y binary alloy due to still dominant compounds at this moment. At ~~elevated at~~ 350 °C, not only binary and ternary compounds were occurred, but also ~~probably~~ there is occurrence of quaternary compounds. Binary compounds that occured are CuSe, Cu_2-Se_x, SnSe. ~~and Cu_3Sn for a ternary compound,~~ In addition there is a formation of ternary and quaternary compound $CuSnSe_3$ and ~~for a quaternary compound is~~ $Cu_2ZnSnSe_4$, respectively. At 450 °C and 550 °C, there are five peaks at 2θ = 17.35°, 27.13°, 36.11°, 45.09°, and 53.45° which can be indexed to (101), (112), (211), (204/220), and (312/116) respectively. These peaks are probably belonging to Cu_2SnSe_3 (ICDD: 01-089-1879) or $Cu_2ZnSnSe_4$ peaks (ICDD: 00-052-0868). In XRD, the difficulty lies in the presence of a secondary phase such as Cu_2SnSe_3 (CTS), which has the same underlying zinc-blende structure (when neglecting the difference between cations) as kesterite or stannite phases of CZTSe. All of these reactions were described in Figure 6.

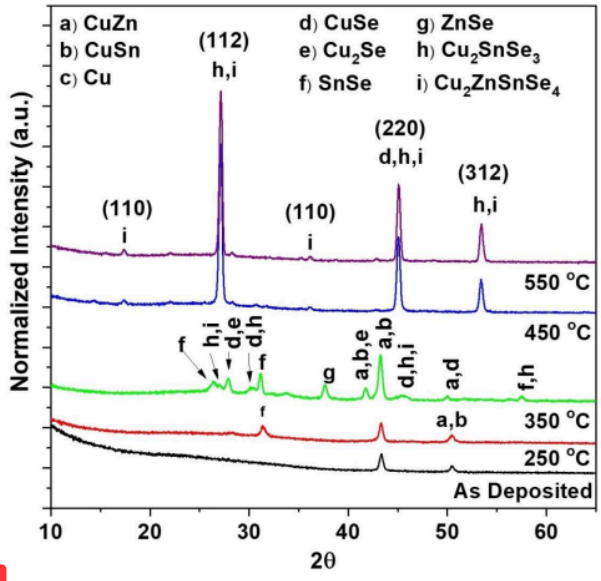

Figure 6. XRD pattern of CZT precursors at elevated selenization temperatures under Ar (95%) + H_2 (5%) for 120 min.

The CZT precursor's reactions involved several reactions that could be divided into primary, binary, ternary, and quaternary reactions. For primary reaction, it consists of a reaction between selenium with H_2, Cu, Zn, and Sn produced binary compounds such as H_2Se, Cu_xSe, ZnSe, and SnSe. Binary reaction happened because some binary compounds such as Cu_xSe, ZnSe, SnSe, CuZn, and CuSn react with H_2Se form a Cu_2SnSe_3 (CTS) as a ternary compound. And finally, a quaternary reaction happened because CTS, as a ternary compound, reacts with ZnSe form a quaternary compound known as $Cu_2ZnSnSe_4$ (CZTSe). All of these reactions are given below. ~~written as:~~

Primary reactions:

$$Se\ (g) + H_2\ (g) \rightarrow H_2Se\ (g) \quad (5)$$

$$Cu\ (s) + H_2Se\ (g) \rightarrow Cu_xSe\ (s) + H_2\ (g) \quad (6)$$

$$Zn\ (s) + H_2Se\ (g) \rightarrow ZnSe\ (s) + H_2\ (g) \quad (7)$$

$$Sn\ (s) + H_2Se\ (g) \rightarrow SnSe\ (s) + H_2\ (g) \quad (8)$$

$$C\ (s) + H_2\ (g) \rightarrow CH_x\ (g) \quad (9)$$

Binary reaction:

$$CO\,(s) + H_2\,(g) \rightarrow CH_x\,(g) + H_2O\,(g) \quad (10)$$

$$CuZn\,(s) + H_2Se\,(g) \rightarrow Cu_xSe\,(s) + ZnSe\,(s) + H_2\,(g) \quad (11)$$

$$CuSn\,(s) + H_2Se\,(g) \rightarrow Cu_xSe\,(s) + SnSe\,(s) + H_2\,(g) \quad (12)$$

Tertiary reactions:

$$CuSe\,(s) + CuSn\,(s) + 2\,H_2Se\,(g) \rightarrow Cu_2SnSe_3\,(s) + 2\,H_2\,(g) \quad (13)$$

$$Cu_2Se\,(s) + SnSe\,(s) + H_2Se\,(g) \rightarrow Cu_2SnSe_3\,(s) + H_2\,(g) \quad (14)$$

$$CuSn\,(s) + H_2Se\,(g) \rightarrow Cu_2SnSe_3\,(s) + H_2\,(g) \quad (15)$$

Quaternary reaction:

$$Cu_2SnSe_3\,(s) + ZnSe\,(s) \rightarrow Cu_2ZnSnSe_4\,(s) \quad (16)$$

To confirm the formation of CZTSe thin film Raman spectroscopy was carried out, in which the selenization was performed at 250 °C, 350 °C, 450 °C, 550 °C, and as CZT precursor. Beside confirming the CZTSe, Raman spectra also used to confirm the carbon existence. At CZT precursor, as an initial phase, there was no peak, but after selenization at 250 °C, one peak occurred at 258 cm^{-1} This peak belongs to the CuSe or Cu_2Se compound, which are products of a reaction between copper in the CZT precursor with selenium in the atmosphere at 250 °C and 350 °C, respectively. At 450 °C, the CZTSe peak at 198 cm^{-1} was started to occur. On the other hand, Raman spectra also exhibits organic residue in carbon compounds as amorphous carbon that as shows a spectrum that has a slope and marked as specific peaks pattern that named as D and G peaks at 1350 cm^{-1} and 1585 cm^{-1}, respectively. Raman spectra shows both D and G peaks were disappeared gradually as elevated temperature. Finally, at 550 °C, Raman spectra shows specific peaks for CZTSe at 174 cm^{-1}, 198 cm^{-1}, and 234 cm^{-1} with no longer D and G peaks were exhibited as shown in the Figure 7. Raman spectra for CZTSe confirmation peaks was shown in the Figure S1 and Raman spectra for carbon residue was shown in the Figure S2.

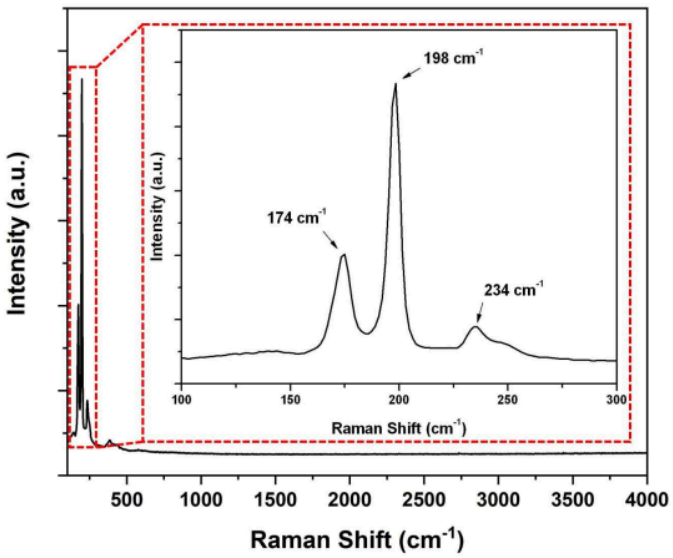

Figure 7. Raman spectrum of CZTSe thin film. Inset shows the expanded view of Raman shift for 100 to 300 cm^{-1}

~~Furthermore,~~ The SEM observation of elevated temperature morphologies and its cross-sectional image is shown in Figure 8. In this figure, the CZT precursor shows small grain morphology. At 250 °C, selenization shows some hexagonal that is indication of ~~to~~ copper selenium (Cu_2-Se_x) compound, and at this condition, SnSe ~~also~~ probably formed in a small amount. At 350 °C selenization, selenium binary compounds such as CuSe, ZnSe, and SnSe can be seen in Figure 8(c), in which CuSe, ZnSe, and SnSe ~~had~~ show hexagonal, tetragonal, and thread-like shape, respectively. The SEM images shown ~~At~~ for 250 °C and 350 °C ~~shows~~ are in consistent ~~consistency~~ with the XRD pattern and Raman spectrum, which shows some presence of binary compounds such as CuSe, Cu_2-Se_x, SnSe, and Cu_3Sn. At 450 °C, it shows a small grain size of CZTSe. However, after elevated selenization temperature ~~until~~ at 550 °C,

the grain size of CZTSe was ~~an~~ increased. At this moment, the CZTSe has been formed well with high crystallinity. This result is consistent with the Raman spectrum result for elevated selenization temperature at 450 °C and 550 °C. At 550 °C, CZTSe has a granular and compact shape with a thickness of approximately 1300 nm.

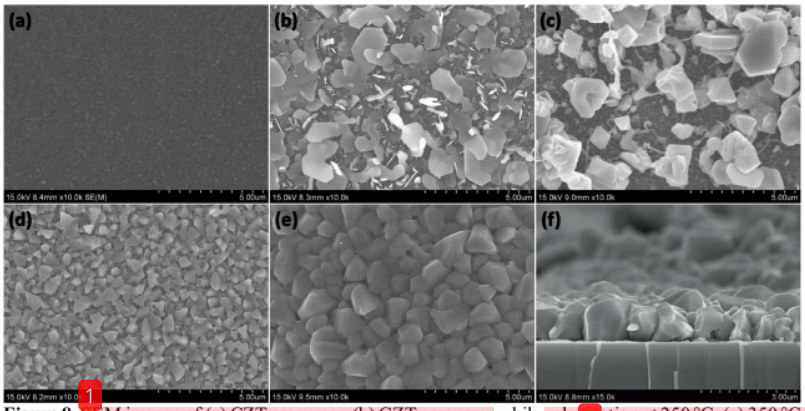

Figure 8. SEM images of (a) CZT precursor, (b) CZT precursor while selenization at 250 °C, (c) 350 °C, (d) 450 °C, and (e) 550 °C and (f) it's cross-section, ~~after selenization under Ar (95%) + H_2 (5%) atmosphere for 120 min~~.

~~Moreover,~~ The chemical composition of CZTSe ~~at elevated temperature~~ was determined by the energy-dispersive x-ray spectroscopy (EDX) at different selenization temperature. At elevated temperature, amount of selenium was increasing because ~~some of~~ compound that containing selenium has been formed, mixed, and accumulated in the thin film. Starting from primary, binary, tertiary, and finally a quaternary compound such as CZTSe was formed. Besides, there are any possibilities of some elements such as tin was evaporated during selenization. As a consequence, the chemical composition of CZTSe was changed during the selenization as shown in the Table S1. Table S1 shows ~~–~~chemical composition change at elevated temperature.

In this work, because determination of chemical composition uses a comparison of intensity from each element in the sample, if the selenium amount in the sample was increased automatically, the other

elements should be decreased although the other elements had fixed chemical composition. Therefore, to determine which element is showing the change, we used the chemical composition ratio approach as well. Usually, Cu/(Zn+Sn), Zn/Sn, and Se/metal ratios are used to described chemical composition in the thin film. However, these ratios are not enough to describe which elements ~~are~~ changes during selenization. From these ratios, we only could know the change for tin and selenium. Thus, to determine the change in copper and zinc ~~change~~ during selenization, Cu/Zn and Cu/Sn ratio should be calculated to describe the change in copper and zinc as well.

Furthermore, the optical properties of CZTSe are determined by the spectrophotometer and the results are shown in Figure 9. The optical properties of CZTSe thin film exhibited a transmittance more than 25% in the infrared range (1200 nm – 2000 nm) and ~~transmittance~~ at visible range (300 – 800 nm) exhibited no transmittance and for direct bandgap value of CZTSe thin film was 1.26 eV, 1.27 eV, 1.27 eV, and 1.29 eV for CZTSe at elevated temperature 250 °C, 350 °C, 450 °C, and 550 °C, respectively.

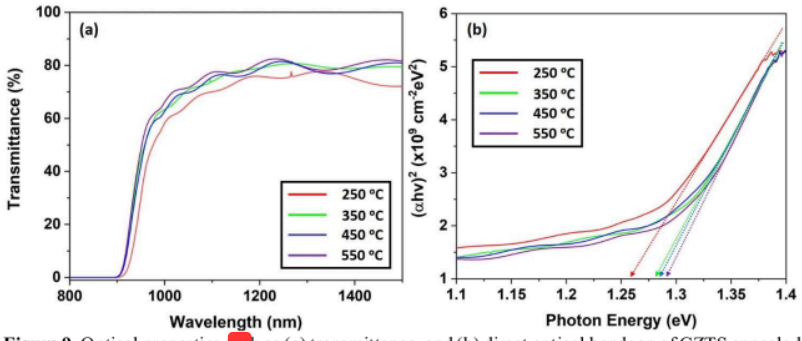

Figure 9. Optical properties such as (a) transmittance, and (b) direct optical bandgap of CZTS annealed at elevated temperature from 250 °C to 550 °C for 120 minutes under Ar (95%) + H_2 (95%) atmosphere, ~~(a) transmittance, and (b) direct optical bandgap~~.

~~Moreover,~~ The electrical properties of CZTSe thin film such as carrier concentration, mobility, conductivity, and resistivity were determined using the Hall measurement apparatus. In this work, electrical properties mostly effected both organic and inorganic phases in the thin film. At 250 °C, the thin film dominated by organic residues and still there is low content of metal selenide compounds.

Thus, CZTSe at this stage has both low carrier concentration and mobility yet, it has a high ~~of~~ resistivity due to carbon residue acts as insulator. Furthermore, at elevated temperature, both carrier concentration and mobility gradually increased, yet resistivity gradually decreased because at 350 °C to 450 °C binary and ternary compound start to form whereas carbon residue gradually disappeared. Finally, at 550 °C, CZTSe has been completely formed and no longer there is any secondary and ternary phases ~~detected~~. Carrier concentration, mobility, and resistivity of CZTSe at elevated temperature are shown in the table 2.

Table 2. Electrical properties of CZT precursor at elevated selenization temperature under Ar (95%) + H_2 (5%) for 120 min.

Temp (°C)	Carrier Concentration (cm^3)	Mobility (cm^2/Vs)	Resistivity (Ωcm)
250	1.72×10^{11}	1.28×10^{-6}	2.55×10^{1}
350	5.70×10^{15}	4.30×10^{-5}	3.25×10^{0}
450	8.26×10^{17}	1.05×10^{0}	3.40×10^{-2}
550	1.75×10^{18}	3.20×10^{0}	6.48×10^{-2}

In order to see its potential as an absorber layer in the solar cell, optical and electrical properties in this work also compared with Kumar and Yakusev's work [31,32] ~~and shows a promising property as an absorber layer in the thin film solar cells.~~

To validate and to pre-investigate the experimental findings, Solar Cell Capacitance Simulator (SCAPS-1D) is used to oversee the performance of proposed $CsPbI_3$/CZTSe based perovskite solar cell. ~~A Solar Cell Capacitance Simulator~~ SCAPS is a one-dimensional computer ~~simulation~~ software for simulating the alternating current and direct current electrical attributes of thin film heterojunction solar cells. Although it was encouraged to study primarily CdTe and CIGS based solar cells, SCAPS is currently used to investigate and validate the characteristics of all types of solar cells with different buffer layers as well. SCAPS-1D software essentially operates on two simple semiconductor equations, such as the Poisson equation and the continuity equation of electrons and holes in steady state which are expressed in equation 5,6 & 7~~..equation number should be changed, as earlier we used 16~~

~~equations/reactions~~. The Poisson equation is:

$$\frac{d^2}{dx^2}\psi(x) = \frac{e}{\varepsilon_0 \varepsilon_r}\left(p(x) - n(x) + N_D - N_A + \rho_p - \rho_n\right) \ldots\ldots\ldots\ldots (5)$$

Here, ψ is electrostatic potential, N_D and N_A are donor and acceptor concentrations, e is electrical charge, ε_r is relative permittivity and ε_0 is the vacuum permittivity, ρ_p and ρ_n are holes and electrons distribution, respectively. The continuity equations for electrons and holes are as following:

$$\frac{dJ_n}{dx} = G - R \ldots\ldots\ldots\ldots (6)$$

$$\frac{dJ_p}{dx} = G - R \ldots\ldots\ldots\ldots (7)$$

Here, J_n and J_p are electron and hole current densities, G is the generation rate, R is the recombination rate. In this paper, we have incorporated the experimental results of CZTSe as an absorber layer of CZTSe/CdS solar cell and proposed i-ZnO/CdS/CZTSe/Mo structure for industrial fabrication. For illumination, a regular AM1.5 G spectrum (1000 W/m^2; T = 300K) was used. Typical thicknesses of each layer were obtained from the different literatures [33-35]. Interface defect layers (IDL) of 10 nm thickness ~~were~~ was used to assess the effect of defect densities subsisting on material interfaces. In addition, the neutral type ~~of~~ defect model is used in simulation where the density of the defect in the active layer has been considered 10^{10} cm^{-3}. The thermal velocity of electrons and holes of 1×10^7 cm/s, the Gaussian energy distribution with a characteristic energy of 0.1 eV have been considered for the model. The schematic structure of the simulated solar cell is shown in Figure 9. Parameters used for this simulation are given in Table 3, 4 & 5.

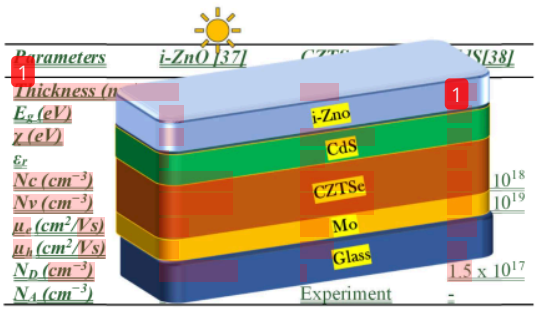

Figure 9: Schematic diagram of CZTSe/CdS solar cell

Table 3: Material Properties Used for simulation

Parameters	i-ZnO [37]	CZTSe [36,39]	CdS[38]
Thickness (nm)	80	1500	100
E_g (eV)	3.3	Experimental	2.4
χ (eV)	4.4	4.55-4.49	4.2
ε_r	9	9.4	10
N_C (cm^{-3})	2.5×10^{18}	2.2×10^{18}	2.2×10^{18}
N_V (cm^{-3})	2.0×10^{19}	1.5×10^{19}	1.8×10^{19}
μ_e (cm^2/Vs)	100	100	100
μ_h (cm^2/Vs)	25	12.5	25
N_D (cm^{-3})	1.0×10^{18}	-	1.5×10^{17}
N_A (cm^{-3})	-	Experiment	-

Table 4: Device parameters used in the simulation

Table 5: Contact material properties used in the simulation

Contact Material Properties			
~~Property~~ ~~Material Properties~~	~~Front contact~~	Back contact	
~~Surface~~ ~~Front contact~~	~~10^7 cm/s~~	~~Back contact~~	10^5 cm/s
~~Surface recombination velocity~~	~~10^7 cm/s~~	~~10^5 cm/s~~	~~10^5 cm/s~~
Surface recombination velocity	10^5 cm/s	10^7 cm/s	10^7 cm/s
~~Surface recombination velocity~~ ~~Simulated Cell Properties~~	~~10^7 cm/s~~	~~10^7 cm/s~~	~~10^7 cm/s~~
~~Cell temperature~~	300 K		
~~Metal work function~~ Majority carrier type	Flat band	Flat band	Mo (5 eV)
~~Metal work function~~	~~Flat band~~	~~Flat band~~	~~Mo (5 eV)~~
Series resistance R_s	2.6 Ωcm^2		
Shunt Resistance R_{sh}	370 Ωcm^2		

From the simulation it has been revealed ~~(fig 10)~~ that, as shown in Figure 10, quantum efficiency (QE)% increases significantly by shifting more towards red region with the increase of CZTSe annealing temperature. However, mild variation in absorbance of light spectrum has been observed when CZTSe annealed at 350ºC ~~and above temperature~~ (Figure 10 inset). It has been found that the proposed CZTSe structure can absorb the sunlight wavelength up to 930 nm when it was annealed at 550ºC.

~~Simulated Cell Properties~~	
~~Cell temperature~~	~~300 K~~
~~Series resistance R_s~~	~~4.25 Ωcm^2~~
~~Shunt Resistance R_{sh}~~	~~370 Ωcm^2~~

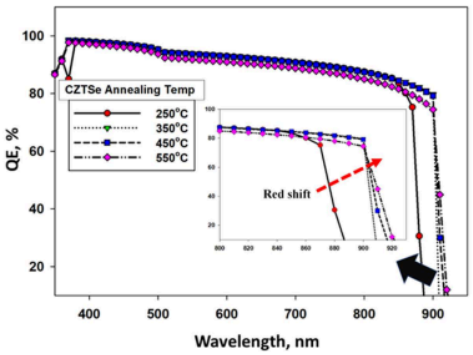

Figure 10: QE% of CZTSe solar cell for differently annealed CZTSe film

Figure 11 reveals that the red shift of QE% has attributed to higher Voc which results the increment of overall efficiency in solar cell. Moreover, it has been found that CZTSe annealing temperature has little impact on Jsc. Highest Jsc of 36.53 mA/cm^2 has been observed for the CZTSe film when annealed at 250°C and lowest 31.55 mA/cm^2 observed for 550°C annealed CZTSe film. On the other hand, highest Voc of 0.95 V has been found for the CZTSe film when annealed at 550°C and lowest 0.42 V observed for 250°C annealed CZTSe film.

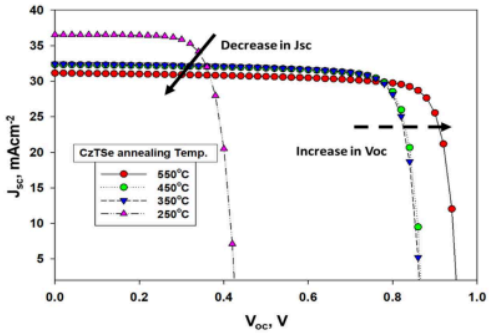

Figure 11: J-V curve of CZTSe solar cell with differently annealed CZTSe film

The increment in Voc and decrement in Jsc with respect to CZTSe annealing temperature has been depicted in Figure 12. Voc has increased due to two factors: change in bandgap and change in carrier concentration. We know that short-circuit current density decreases with increasing bandgap, the open-circuit voltage increases as the band gap increases. In this experiment, bandgap of CZTSe has increased with the annealing temperature which attributed to increase in Voc and decrease in Jsc.

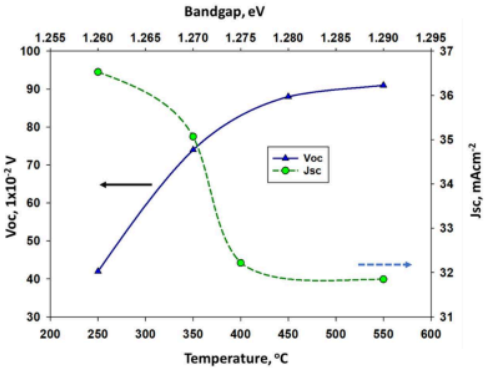

Figure 12: Relationship between Voc and Jsc with CZTSe annealing temperature~~, in the x-axis~~

~~label.., mention annealing temperature..~~

Again, Voc has a significant relation with carrier concertation which is expressed in equation 8.~~..equation no should be in different..:~~

$$v_{0c} = \frac{kT}{q} ln\left[\frac{(N_A+\Delta n)\Delta n}{n_i^2}\right] \ldots\ldots\ldots\ldots\ldots\ldots(8)$$

where kT/q is the thermal voltage, N_A is the doner concentration, Δn is the excess carrier concentration and n_i is the intrinsic carrier concentration. It determines that Voc increases with the increase of donor concentration while other factors are constant. In our experiment we observed that CZTSe carrier concentration has increased with the increase of annealing temperature, that also contributed to increase of Voc of the device. The proposed i-ZnO/CdS/CZTSe based solar cell exhibits highest efficiency of 23.88% with Voc= 0.95 V, Jsc= 31.55 mA/cm^2 and FF= 82.80% while CZTSe thin film annealed at 550°C. Hence, it can be said that the experimental results are valid and hence, this study proposes 550°C annealed CZTSe thin film to be incorporated as absorber layer in the proposed structure.

Table 6: Comparison with similar reported solar cell

Cell Structure	*Voc (V)*	*Jsc (mAcm^{-2})*	*FF (%)*	*Efficiency (%)*	*Year*	*Ref*
CZTSe/CdS	0.513	35.2	69.8	12.6	2014	[40]
CZTSe/CdS	0.41	37.27	73.79	11.43	2019	[41]
CZTSe/CdS	0.38	35.36	59.9	8.2	2016	[42]
CZTSe/CdS	0.95	31.55	82.80	**23.88**	2021	This experiment

Table 6 expresses the comparative study with other reported results of similar device structure. It is revealed that our study paves the way for achieving higher Voc compared to other reported study which can push forward the CZTSe solar cell photovoltaic efficiency upto 23.88%.

Conclusions

$Cu_2ZnSnSe_4$ (CZTSe) was prepared by the CZT precursor, deposited from the metal-ethanolamine complex compound without hydrazine addition selenization. The best condition for selenization is under Ar (95%) + H_2 (5%) at 550 °C for 120 minutes. After selenization at 550 °C, the CZT precursor was completely grown into CZTSe with a compact granular shape and approximately 1300 nm of thickness. Organic impurities were disappeared gradually due to the effect of elevated temperature and atmospheric effect. During selenization, the selenium amount in the CZTSe was increasing gradually due to selenium was react with the CZT precursor. On the other hand, the tin amount was decreased gradually due to tin evaporation. It was the easiest element to evaporate among copper and zinc compound conditions. The composition was changed at elevated selenization temperature. However, organic impurities from organic residue were disappeared gradually under 450 °C. At 550 °C as the best condition of selenization condition, CZTSe has 1.29 eV, showing p-type of semiconductor, and has carrier concentration, mobility, and resistivity as 1.75×10^{18} cm^3, 3.20 cm^2/Vs, 6.48 $\times10^{-2}$ Ωcm, respectively and its suitable for absorber layer solar cells. Finally, numerical simulation validates the incorporation of 550ºC annealed CZTSe thin film as can absorber layer and suggests that careful fabrication of full device can give a major breakthrough of CZTSe solar cell which can exhibit the cell efficiency up to 23.88%.

Acknowledgment

This paper tributed to Prof. Kim Kyoo Ho as the author's supervisor (Ersan) in Yeungnam University for his kindness as the last paper before the retirement. This study was supported by the Basic Science

Research Program (2013R1A1A2013408) and Center for Inorganic Photovoltaic Materials (No.2012-0001170) through the National Research Foundation of Korea (NRF) funded by the Ministry of Science, ICT and Future Planning. Authors also extended their appreciation to The University Researchers Supporting Project Number (TURSP-2020/264), Taif University, Taif, Saudi Arabia. Thanks to the Ministry of Education and Culture of the Republic of Indonesia and all collaborators from the University of Indonesia and Kanazawa University, and The National University of Malaysia through the research grant support with code RS 2018-003. The authors gratefully acknowledge to Dr. Marc 394 Bargeman, University of Gent, Belgium, for providing the SCAPS simulation software.

References

[1] Yan, C., Huang, J., Sun, K., Johnston, S., Zhang, Y., Sun, H., ... & Yang, L. (2018). Cu 2 ZnSnS 4 solar cells with over 10% power conversion efficiency enabled by heterojunction heat treatment. Nature Energy, 3(9), 764-772.

[2] Zhang, Z., Gao, Q., Guo, J., Zhang, Y., Han, Y., Ao, J., ... & Zhang, Y. (2020). Over 10% Efficient Pure CZTSe Solar Cell Fabricated by Electrodeposition with Ge Doping. Solar RRL, 4(5), 2000059.

[3] Wang, W., Winkler, M. T., Gunawan, O., Gokmen, T., Todorov, T. K., Zhu, Y., & Mitzi, D. B. (2014). Device characteristics of CZTSSe thin-film solar cells with 12.6% efficiency. Advanced Energy Materials, 4(7), 1301465.

[4] David B. Mitzi, Oki Gunawan, Teodor K. Todorov, Kejia Wang, Supratik Guha. Solar Energy Materials and Solar Cells 95 (2011) 1421-1436.

[5] T.K. Todorov, J. Tang, S. Bag, O. Gunawan, T. Gokmen, Y.Zhu, D.B. Mitzi, Beyond 11% efficiency: characteristics of state-of-the-art $Cu_2ZnSn(S,Se)_4$ solar cells, Advanced Energy Materials 3 (2012) 34-38.

[6] Muslih, E. Y., & Kim, K. H. (2015). Characteristics of Cu2ZnSnS4 thin film prepared by

calcination and sulfurizing of metal (Cu, Zn, Sn)-ethanolamine precursor complexed from metal (Cu, Zn, Sn)-hydrate. Chalcogenide Lett, 12, 349-355.

[7] Amal, M. I., & Kim, K. H. (2013). Structural and optical properties of sulfurized Cu 2 ZnSnS 4 thin films from Cu–Zn–Sn alloy precursors. Journal of Materials Science: Materials in Electronics, 24(2), 559-566.

[8] Munir, B., Prastyo, B. E., Muslih, E. Y., & Nurjaya, D. M. (2016). Non-sulfurization Single Solution Approach to Synthesize CZTS Thin Films. International Journal of Technology, 7(8), 1326-1334.

[9] Todorov, T., Kita, M., Carda, J., & Escribano, P. (2009). Cu2ZnSnS4 films deposited by a soft-chemistry method. Thin Solid Films, 517(7), 2541-2544.

[10] Sun, Y., Zhang, Y., Wang, H., Xie, M., Zong, K., Zheng, H., ... & Lau, W. (2013). Novel non-hydrazine solution processing of earth-abundant Cu 2 ZnSn (S, Se) 4 absorbers for thin-film solar cells. Journal of Materials Chemistry A, 1(23), 6880-6887.

[11] Y.E. Romanyuk, C.M. Fella, A.R. Uhl, M. Werner, A.N. Tiwari, T. Schnabel, E. Ahlswede. Solar Energy Materials and Solar Cells 119 (2013) 181-189.

[12] Todorov, T., & Mitzi, D. B. (2010). Direct liquid coating of chalcopyrite light-absorbing layers for photovoltaic devices. European Journal of Inorganic Chemistry, 2010(1), 17-28.

[13] Ming-Hung Chiang, Yaw-Shyan Fu, Cheng-Hung Shih, Chun-Cheng Kuo, Tzung-Fang Guo, Wen-Tai Lin. Thin Solid Films 544 (2013) 291-295.

[14] Byungha Shin, Oki Gunawan, yu Zhu, Nestor A. Bojarrczuk, S. Jay Chey and Supratik Guha. Prog. Photovolt: Res. Appl. 21 (2013) 72-76.

[15] Qijie Guo, Grayson M. Ford, Wei-Chang Yang, Bryce C. Walker, Eric A. Stach, Hugh W. Hillhouse, and Rakesh Agrawal. J. Am. Chem. Soc. 132 (2010) 17384–17386.

[16] Teodor Todorov, Oki Gunawan, S. Jay Chey, Thomas Goislard de Monsabert, Aparna Prabhakar, David B. Mitzi. Thin Solid Films 519 (2011) 7378-7381.

[17] Roe, F. J. C., Grant, G. A., & Millican, D. M. (1967). Carcinogenicity of hydrazine and 1, 1-dimethylhydrazine for mouse lung. Nature, 216(5113), 375-376.

[18] Kush, P., & Deka, S. (2014). Photoelectrical properties of surfactant-free kesterite Cu 2 ZnSnSe 4 hydrophilic nanocrystal ink and the stability in polar solvents. Journal of nanoparticle research, 16(9), 2600.

[19] Ritchie, C., Chesman, A. S. R., Jasieniak, J., & Mulvaney, P. (2019). Aqueous synthesis of Cu2ZnSnSe4 nanocrystals. Chemistry of Materials, 31(6), 2138-2150.

[20] Valls, R. M., Lyubenova, T. S., Roures, I. C., Oliveira, L., Chiva, D. F., & Castelló, J. B. C. (2017). Easy and low-cost aqueous precipitation method to obtain Cu2ZnSn (S, Se) 4 thin layers. Solar Energy Materials and Solar Cells, 161, 432-438.

[21] Tan, L., Zhang, Y., Chen, Y., & Chen, Y. (2015). Homogeneous Cu2ZnSnSe4 nanocrystals/graphene oxide nanocomposites as hole transport layer for polymer solar cells. Chemical Physics Letters, 622, 1-8.

[22] Wang, J. J., Hu, J. S., Guo, Y. G., & Wan, L. J. (2012). Wurtzite Cu 2 ZnSnSe 4 nanocrystals for high-performance organic–inorganic hybrid photodetectors. NPG Asia Materials, 4(1), e2-e2.

[23] Shibayama, N., Zhang, Y., Satake, T., & Sugiyama, M. (2017). Modelling of an equivalent circuit for Cu 2 ZnSnS 4-and Cu 2 ZnSnSe 4-based thin film solar cells. RSC Advances, 7(41), 25347-25352.

[24] Sampath, S., Uchida, H., & Yoneyama, H. (1994). Photocatalytic degradation of gaseous pyridine over zeolite-supported titanium dioxide. Journal of Catalysis, 149(1), 189-194.

[25] Berglund, B., Höglund, A., & Esfandabad, H. S. (2012). A bisensory method for odor and irritation detection of formaldehyde and pyridine. Chemosensory Perception, 5(2), 146-157.

[26] Ito, N., Hasegawa, R., Imaida, K., Tamano, S., Hagiwara, A., Hirose, M., & Shirai, T. (1997). Carcinogenicity of 2-amino-1-methyl-6-phenylimidazo [4, 5-b] pyridine (PhIP) in the rat. Mutation Research/Fundamental and Molecular Mechanisms of Mutagenesis, 376(1-2), 107-114.

[27] Cho, A., Song, H., Gwak, J., Eo, Y. J., Yun, J. H., Yoon, K., & Ahn, S. (2014). A chelating effect in hybrid inks for non-vacuum-processed CuInSe 2 thin films. Journal of Materials Chemistry A, 2(14), 5087-5094.

[28] Dimitrievska, M., Fairbrother, A., Saucedo, E., Pérez-Rodríguez, A., & Izquierdo-Roca, V. (2016). Secondary phase and Cu substitutional defect dynamics in kesterite solar cells: impact on optoelectronic properties. Solar Energy Materials and Solar Cells, 149, 304-309.

[29] Olgar, M. A., Atasoy, Y. A. V. U. Z., Başol, B. M., Tomakin, M., Aygun, G., Ozyuzer, L., & Bacaksız, E. (2016). Influence of copper composition and reaction temperature on the properties of CZTSe thin films. Journal of Alloys and Compounds, 682, 610-617.

[30] Just, J., Sutter-Fella, C. M., Lützenkirchen-Hecht, D., Frahm, R., Schorr, S., & Unold, T. (2016). Secondary phases and their influence on the composition of the kesterite phase in CZTS and CZTSe thin films. Physical Chemistry Chemical Physics, 18(23), 15988-15994.

[31] Wibowo, R. A., Yoo, H., Hölzing, A., Lechner, R., Jost, S., Palm, J., ... & Hock, R. (2013). A study of kesterite Cu2ZnSn (Se, S) 4 formation from sputtered Cu–Zn–Sn metal precursors by rapid thermal processing sulfo-selenization of the metal thin films. Thin Solid Films, 535, 57-61.

[32] Kumar, V., Dutta, A., & Singh, U. P. (2020). Optimization of selenization parameters for fabrication of CZTSe thin film. Superlattices and Microstructures, 106578.

[33] K. Sobayel, Md. Akhtaruzzaman, et. al. (2019). A comprehensive defect study of tungsten disulfide (WS2) as electron transport layer in perovskite solar cells by numerical simulation. Results in Physics, Volume 12, Pages 1097-1103.

[34] K. Sobayel, N. Amin, et. al. (2020). Efficiency enhancement of CIGS solar cell by WS2 as window layer through numerical modelling tool. Solar Energy, Volume 207, 2020.

[35] K. Sobayel et. al. (2018). Numerical modelling on prospective buffer layers for tungsten di-sulfide (WS2) solar cells by scaps-1d. Chalcogenide Letters, Vol. 15, No. 6, p. 307 – 315.

[36] Yakushev, M. V., Sulimov, M. A., Márquez-Prieto, J., Forbes, I., Krustok, J., Edwards, P. R. &

Martin, R. W. (2017). Influence of the copper content on the optical properties of CZTSe thin films. Solar Energy Materials and Solar Cells, 168, 69-77.

[37] G. Kartopu, B.L. Williams, V. Zardetto, A.K. Gürlek, A.J. Clayton, S. Jones, W.M.M. Kessels, M. Creatore, S.J.C. Irvine, Enhancement of the photocurrent and efficiency of CdTe solar cells suppressing the front contact reflection using a highly-resistive ZnO buffer layer, Solar Energy Materials and Solar Cells, Volume 191, 2019, Pages 78-82.

[38] F.T. Munna, Vidhya Selvanathan, K. Sobayel, et al., Diluted chemical bath deposition of CdZnS as prospective buffer layer in CIGS solar cell, Ceramics International, 2020.

[39] Khattak, Y.H., Baig, F., Toura, H. *et al.* CZTSe Kesterite as an Alternative Hole Transport Layer for $MASnI_3$ Perovskite Solar Cells. *Journal of Elec Material* **48,** 5723–5733 (2019). https://doi.org/10.1007/s11664-019-07374-5

[40] Wang, Wei; Winkler, Mark T.; Gunawan, Oki; Gokmen, Tayfun; Todorov, Teodor K.; Zhu, Yu; Mitzi, David B. (2014). Device Characteristics of CZTSSe Thin-Film Solar Cells with 12.6% Efficiency. Advanced Energy Materials, 4(7), n/a–n/a. doi:10.1002/aenm.201301465.

[41] Li, Xinchen; Zhuang, Daming; Zhang, Ning; Zhao, Ming; Yu, Xinping; Liu, Peng; Wei, Yaowei; Ren, Guoan (2019). Achieving 11.95% efficient CuZnSnSe solar cells fabricated by sputtering Cu-Zn-Sn-Se quaternary compound target with selenization process. Journal of Materials Chemistry A. doi:10.1039/C9TA00385A

[42] Liyong Yao, Jianping Ao, Ming-Jer Jeng, Jinlian Bi, Shoushuai Gao, Guozhong Sun, Qing He, Zhiqiang Zhou, Yun Sun, Liann-Be Chang, A CZTSe solar cell with 8.2% power conversion efficiency fabricated using electrodeposited Cu/Sn/Zn precursor and a three-step selenization process at low Se pressure, Solar Energy Materials and Solar Cells, Volume 159, 2017.

4626_4DlHsul7XCIQcIZIHmx4.docx

ORIGINALITY REPORT

39%
SIMILARITY INDEX

PRIMARY SOURCES

1	Ersan Y. Muslih, Khan Sobayel Bin Rafiq, Mohammad Ismail Hossain, Md. Shahiduzzaman et al. "Growth and reaction mechanism of solution-processed Cu2ZnSnSe4 thin films for realising efficient photovoltaic applications", Journal of Alloys and Compounds, 2022 Crossref	1559 words — 23%
2	F.T. Munna, Vidhya Selvanathan, K. Sobayel, Ghulam Muhammad, Nilofar Asim, Nowshad Amin, Kamaruzzaman Sopian, Md. Akhtaruzzaman. "Diluted chemical bath deposition of CdZnS as prospective buffer layer in CIGS solar cell", Ceramics International, 2020 Crossref	132 words — 2%
3	scholar.ui.ac.id Internet	127 words — 2%
4	www.mdpi.com Internet	111 words — 2%
5	ijred.cbiore.id Internet	46 words — 1%
6	iopscience.iop.org Internet	42 words — 1%
7	www.beilstein-journals.org Internet	

36 words — 1%

8	pdffox.com Internet	27 words — < 1%
9	www.ncbi.nlm.nih.gov Internet	27 words — < 1%
10	Shreyash Hadke, Menglin Huang, Chao Chen, Ying Fan Tay, Shiyou Chen, Jiang Tang, Lydia Wong. "Emerging Chalcogenide Thin Films for Solar Energy Harvesting Devices", Chemical Reviews, 2021 Crossref	26 words — < 1%
11	M.K. Sobayel, M.S. Chowdhury, T. Hossain, H.I. Alkhammash et al. "Efficiency enhancement of CIGS solar cell by cubic silicon carbide as prospective buffer layer", Solar Energy, 2021 Crossref	25 words — < 1%
12	www.researchgate.net Internet	24 words — < 1%
13	Narjes Beigom Mortazavi Amiri, Andrei Postnikov. " Secondary phase Cu SnSe vs. kesterite Cu ZnSnSe : Similarities and differences in lattice vibration modes ", Journal of Applied Physics, 2012 Crossref	20 words — < 1%
14	Badrul Munir, Ersan Y. Muslih. "Novel Synthesis of ZnOThin Films by Facile Solution Process", Journal of King Saud University - Engineering Sciences, 2020 Crossref	19 words — < 1%
15	renewableenergybusiness.info Internet	18 words — < 1%

16	ejournal.upi.edu Internet	17 words — < 1%
17	www.european-mrs.com Internet	17 words — < 1%
18	Qing Zhou, Junhui Hei, Jiahui Ma, Zihang Liu et al. "Controllable in situ sodium doping induces uniform nucleation of self-supplied selenium precursor enables large-grain spanning kesterite absorber", Chemical Engineering Journal, 2025 Crossref	16 words — < 1%
19	K. Nurhafiza, P. Chelvanathan, Md Khan Sobayel Bin Rafiq, F.T. Munna et al. "Effect of Cd2+ Molar Concentration in CdxZn(1-x)S Thin Film by Chemical Bath Deposition Technique Using Alternative Sulfur Precursor", ECS Journal of Solid State Science and Technology, 2021 Crossref	14 words — < 1%
20	Khadka, Dhruba B., SeongYeon Kim, and Junho Kim. "A Non-Vacuum Approach for Fabrication of Cu2ZnSnSe4/In2S3 Thin Film Solar Cell and Opto-Electronic Characterization", The Journal of Physical Chemistry C Crossref	14 words — < 1%
21	Naoufal Ennouhi, Yassine Chouimi, Noureddine Ben Afkir, Abdeljalile Er-rfyg, Sanaa Ammari, Massaab El Ydrissi, Zouheir Sekkat. "Silver and sodium incorporation into wide bandgap CZTS absorbers on transparent back electrodes and their application in kesterite/c-silicon tandem solar cells: Experiments and simulations", Solar Energy, 2025 Crossref	14 words — < 1%
22	ir.library.osaka-u.ac.jp Internet	14 words — < 1%

23	E. M. Mkawi, K. Ibrahim, M. K. M. Ali, K. M. A. Saron, M. A. Farrukh, Nageh K. Allam. "Influence of substrate temperature on the properties of electrodeposited kesterite Cu2ZnSnS4 (CZTS) thin films for photovoltaic applications", Journal of Materials Science: Materials in Electronics, 2014 Crossref	12 words — < 1%
24	Samiya Mahjabin, Md. Mahfuzul Haque, Sobayel Khan, Vidhya Selvanathan et al. "Effects of oxygen concentration variation on the structural and optical properties of reactive sputtered WOx thin film", Solar Energy, 2021 Crossref	12 words — < 1%
25	coek.info Internet	12 words — < 1%
26	jnep.sumdu.edu.ua Internet	12 words — < 1%
27	Fangyang Liu, Fangqin Zeng, Ning Song, Liangxing Jiang et al. " Kesterite Cu ZnSn(S,Se) Solar Cells with beyond 8% Efficiency by a Sol–Gel and Selenization Process ", ACS Applied Materials & Interfaces, 2015 Crossref	11 words — < 1%
28	datapdf.com Internet	11 words — < 1%
29	link.springer.com Internet	11 words — < 1%
30	udspace.udel.edu Internet	11 words — < 1%

31	M. Mottakin, K. Sobayel, Dilip Sarkar, Hend Alkhammash et al. "Design and Modelling of Eco-Friendly CH3NH3SnI3-Based Perovskite Solar Cells with Suitable Transport Layers", Energies, 2021 Crossref	10 words — < 1%
32	Sekou Mariama Camara, Lingling Wang, Xintong Zhang. " Easy hydrothermal preparation of Cu ZnSnS (CZTS) nanoparticles for solar cell application ", Nanotechnology, 2013 Crossref	10 words — < 1%
33	eprints.qut.edu.au Internet	10 words — < 1%
34	Suryawanshi, Mahesh P., Uma V. Ghorpade, Seung Wook Shin et al. "A Simple Aqueous Precursor Solution Processing of Earth-abundant Cu2SnS3 Absorbers for Thin-film Solar Cells", ACS Applied Materials & Interfaces Crossref	9 words — < 1%
35	chalcogen.ro Internet	9 words — < 1%
36	depositonce.tu-berlin.de Internet	9 words — < 1%
37	eprints.undip.ac.id Internet	9 words — < 1%
38	riunet.upv.es Internet	9 words — < 1%
39	www.freepatentsonline.com Internet	9 words — < 1%

40 Nicholas Rono, Abdelkrim E. Merad, Joshua K. Kibet, Bice S. Martincigh, Vincent O. Nyamori. "A theoretical investigation of the effect of the hole and electron transport materials on the performance of a lead-free perovskite solar cell based on CH3NH3SnI3", Journal of Computational Electronics, 2021
Crossref
8 words — < 1%

41 Samer H. Zyoud, Ahed H. Zyoud, Naser M. Ahmed, Atef F. I. Abdelkader. "Numerical Modelling Analysis for Carrier Concentration Level Optimization of CdTe Heterojunction Thin Film–Based Solar Cell with Different Non–Toxic Metal Chalcogenide Buffer Layers Replacements: Using SCAPS–1D Software", Crystals, 2021
Crossref
8 words — < 1%

42 Shrikaant Kulkarni, Hemantkumar N. Akolkar, Vijay M. Khedkar, Rajesh Ramasamy, Kirti R. Mahanwar, Nirmala R. Darekar. "Biogenic-Based Metal Nanomaterials for Sustainable Engineering Applications", Apple Academic Press, 2025
Publications
8 words — < 1%

43 d-nb.info
Internet
8 words — < 1%

44 diglib.tugraz.at
Internet
8 words — < 1%

45 lirias.kuleuven.be
Internet
8 words — < 1%

46 pubs.rsc.org
Internet
8 words — < 1%

47 repositori.uji.es
Internet
8 words — < 1%

48	thesis.univ-biskra.dz Internet	8 words — < 1%
49	N Z Calderon, J L Ampuero, A La Rosa-Toro, B R Pujada. "Influence of substrate temperature on the properties of Ag-C films produced by DC Magnetron Sputtering", Journal of Physics: Conference Series, 2018 Crossref	7 words — < 1%
50	Riolino, I.. "Monte-Carlo simulation of decananometric nMOSFETs: Multi-subband vs. 3D-electron gas with quantum corrections", Solid State Electronics, 200711 Crossref	7 words — < 1%
51	Susan Schorr, Galina Gurieva, Maxim Guc, Mirjana Dimitrievska et al. "Point defects, compositional fluctuations, and secondary phases in non-stoichiometric kesterites", Journal of Physics: Energy, 2019 Crossref	7 words — < 1%
52	"Advanced Characterization Techniques for Thin Film Solar Cells", Wiley, 2016 Crossref	6 words — < 1%
53	Cameron Ritchie, Anthony Sidney Richard Chesman, Jacek Jasieniak, Paul Mulvaney. " Aqueous Synthesis of Cu ZnSnSe Nanocrystals ", Chemistry of Materials, 2019 Crossref	6 words — < 1%
54	Ersan Y. Muslih, Khan Sobayel Bin Rafiq, Mohammad Ismail Hossain, Shahiduzzaman et al. "Growth and Reaction Mechanism of Solution-processed Cu2ZnSnSe4 Thin Films for Realising Efficient Photovoltaic Applications", Journal of Alloys and Compounds, 2021 Crossref	6 words — < 1%

EXCLUDE QUOTES	ON	EXCLUDE SOURCES	OFF
EXCLUDE BIBLIOGRAPHY	ON	EXCLUDE MATCHES	OFF